Pergamon

Bioorganic & Medicinal Chemistry, Vol. 5, No. 12, pp 2193–2201, 1997

PII: S0968-0896(97)00173-9
0968-0896/97 $17.00 + 0.00

Bioactive Conformation of a Potent Stromelysin Inhibitor Determined by X-nucleus Filtered and Multidimensional NMR Spectroscopy

Nina C. Gonnella,* Yu-Chin Li, Xiaolu Zhang and C. Gregory Paris
Novartis Pharmaceuticals Corp., 556 Morris Ave., Summit, NJ 07901 U.S.A.

Abstract—The biologically active conformation of a novel, very potent, nonpeptidic stromelysin inhibitor was determined by X-nucleus filtered and multidimensional NMR spectroscopy. This bound conformer was subsequently docked into the stromelysin catalytic domain (SCD) using intermolecular distance constraints derived from NOE data. The complex showed the S1′ pocket of stromelysin to be the major site of enzyme–inhibitor interaction with other portions of the inhibitor spanning the S2′ and S1 binding sites. Theoretical predictions of SCD-inhibitor binding from molecular modeling studies were consistent with the NMR data. Comparison of modeled enzyme–inhibitor complexes for stromelysin and collagenase revealed an alternate binding mode for the inhibitor in collagenase, suggesting a similar binding interaction might also be possible for stromelysin. The NMR results, however, revealed a single SCD-inhibitor binding mode and provided a structural template for the design of more potent stromelysin inhibitors. © 1997 Elsevier Science Ltd.

Introduction

Stromelysin-1 is a 57 kDa zinc metalloendoproteinase (MMP-3) that is secreted by synoviocytes and articular chondrocytes in response to inflammatory mediators such as interleukin-1.[1] This enzyme is believed to cause the destruction of cartilage proteoglycans associated with osteo- and rheumatoid arthritis[2] and has been implicated in tumor invasion and metastasis.[3,4] Because of stromelysin's link to cartilage degradation, it is anticipated that the design of stromelysin inhibitors could result in the next major class of drugs for the treatment of arthritis.

Studies on the mechanism of action of stromelysin have led to the discovery of C terminally heterogeneous forms of this enzyme of approximately 29 kDa, retaining full biological activity.[5–9] Based on this observation, direct expression of C-terminally truncated human fibroblast prostromelysin was carried out, which was subsequently activated to produce a 20 kDa (173 residue) catalytic domain of the enzyme.[10] The size and purity of this truncated domain have made it amenable for structure elucidation by both NMR spectroscopy and X-ray crystallography.

*Author to whom correspondence should be addressed; Nina C. Gonnella, Novartis Pharmaceuticals Corp., 556 Morris Ave., Summit, NJ 07901, U.S.A. Phone: (908) 277-7265; Fax: (908) 277-2405; E-mail: nina.gonnella@pharma.novartis.com
Key words: stromelysin catalytic domain, nonpeptidic inhibitor, bioactive conformation, NMR spectroscopy.

Several three-dimensional structures of the inhibited catalytic domain of C-truncated stromelysin have been solved either by X-ray or NMR methods.[11–16] The inhibitors used in these studies were dipeptidic or tripeptidic in nature, spanning the S1′ to S3′ subsites in an extended conformation. From a rational drug design standpoint, these studies provided valuable structural information on the size, shape, and chemical composition of the enzyme's binding pocket. This structural information, combined with molecular modeling methods, could be used to predict theoretical binding modes for a variety of different inhibitors. Drawbacks of this approach, however, may arise when two or more binding modes are energetically feasible or when modeling parameters do not sufficiently account for the enzyme dynamics associated with the binding process.[17] To address this uncertainty, NMR spectroscopic methods were employed to determine the bound conformations of stromelysin inhibitors as well as to provide information on key enzyme–inhibitor interactions. Such studies can lead to the facile elucidation of the correct binding mode of an inhibitor prior to generation of the full three dimensional structure of the enzyme–inhibitor complex.

Here we report the first biologically active conformation of a very potent, nonpeptidic stromelysin inhibitor **1** (CGS 27023)[18] obtained from X-nucleus filtered NMR spectroscopy (Fig. 1). The bound conformation of compound **1** was subsequently docked into a reported stromelysin structure,[12] using NOE distance constraints derived from X-nucleus filtered and multidimensional NMR experiments to orient the inhibitor within the binding site. The results showed the S1′ pocket of

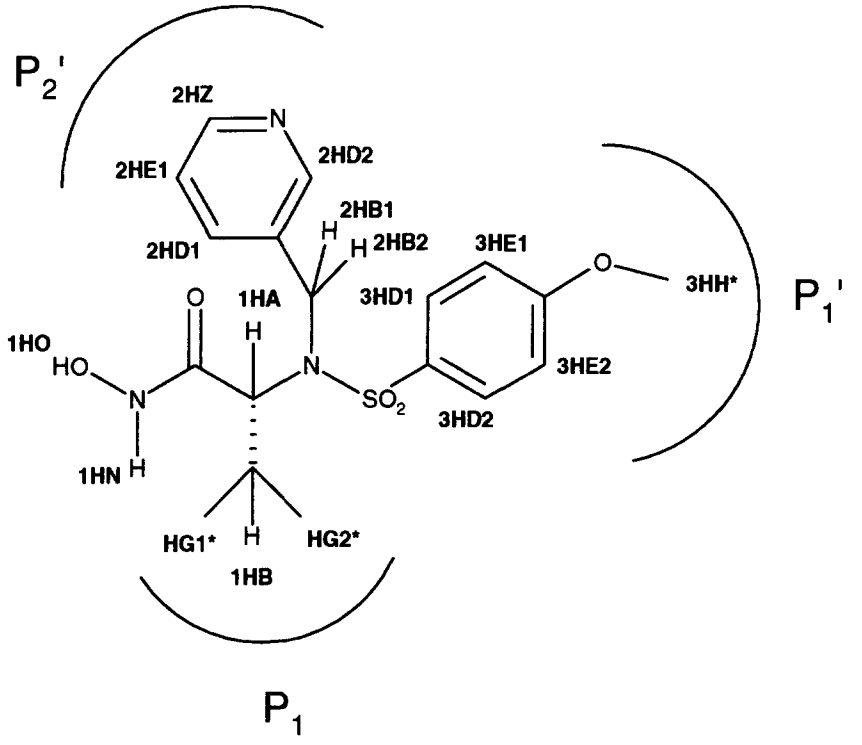

Figure 1. Illustration of the hydroxamic acid inhibitor (**1**, CGS 27023) of the catalytic domain of stromelysin. Schematic representation of the binding mode shows the P1′, P2′ and P1 substituents. This compound has a K_i of 12 nM against stromelysin and a K_i of 31 nM for human fibroblast collagenase.

stromelysin to be the major site of enzyme–inhibitor interaction with minor protein-inhibitor interactions clustered in the S2′ and S1 pockets. The data unequivocally established the binding mode of this inhibitor.

Results and Discussion

Determination of the bioactive conformation of CGS 27023 (1) complexed to SCD

The SCD-inhibitor complex was prepared from the catalytic domain of $^{13}C/^{15}N$ labeled stromelysin and nonlabeled inhibitor with buffer pH adjusted to 6.8 to mimic assay conditions. Initial samples of the complex contained a twofold excess of inhibitor that produced two sets of chemical shifts, corresponding to the bound and free states. A stoichiometric complex was subsequently prepared by buffer exchange using centricon filtration, which allowed a chemical shift distinction between the free and bound states. Chemical shift assignments for the free and bound inhibitor, obtained from X-nucleus filtered COSY experiments, are shown in Table 1. Examination of the data shows chemical shifts of inhibitor protons 2HB1 and 2HB2, and HG1* and HG2* are nonequivalent in the bound state yet degenerate for the free moiety, indicating conformational flexibility of the free inhibitor in solution. Protons on the methoxy phenyl ring were degenerate for 3HD* and 3HE* in both the bound and free states, suggesting that the phenyl ring is rapidly rotating even when complexed to the enzyme. Inhibitor protons [1HN] and [1HO] are visible in the bound state indicating that they are either hydrogen bonded, or protected, and do not rapidly exchange with water. These protons were unambiguously assigned from undecoupled NOESY spectra, where an absence of heteronuclear coupling for the corresponding NOE cross peaks provided clear distinction between proton resonances from the labeled protein and those on the unlabeled inhibitor.

The bound conformation of **1** was calculated from 32 intramolecular NOE distance constraints obtained from $^{13}C/^{15}N$-filtered NOESY experiments (Fig. 2). These

Table 1. Chemical shifts of bound vs. free inhibitor (**1**)

Proton	Bound (ppm)	Free (ppm)
1HN	11.82	—
1HO	14.57	—
1HA	4.55	3.94
1HB	2.36	2.11
HG1*	0.87	0.79
HG2*	1.08	0.79
2HB1	4.97	4.74
2HB2	4.53	4.74
2HD1	8.19	7.68
2HE1	7.51	7.28
2HZ	8.53	8.33
2HD2	8.59	8.32
3HD1/2	7.71	7.52
3HE1/2	6.96	6.95
3HH*	3.96	3.83

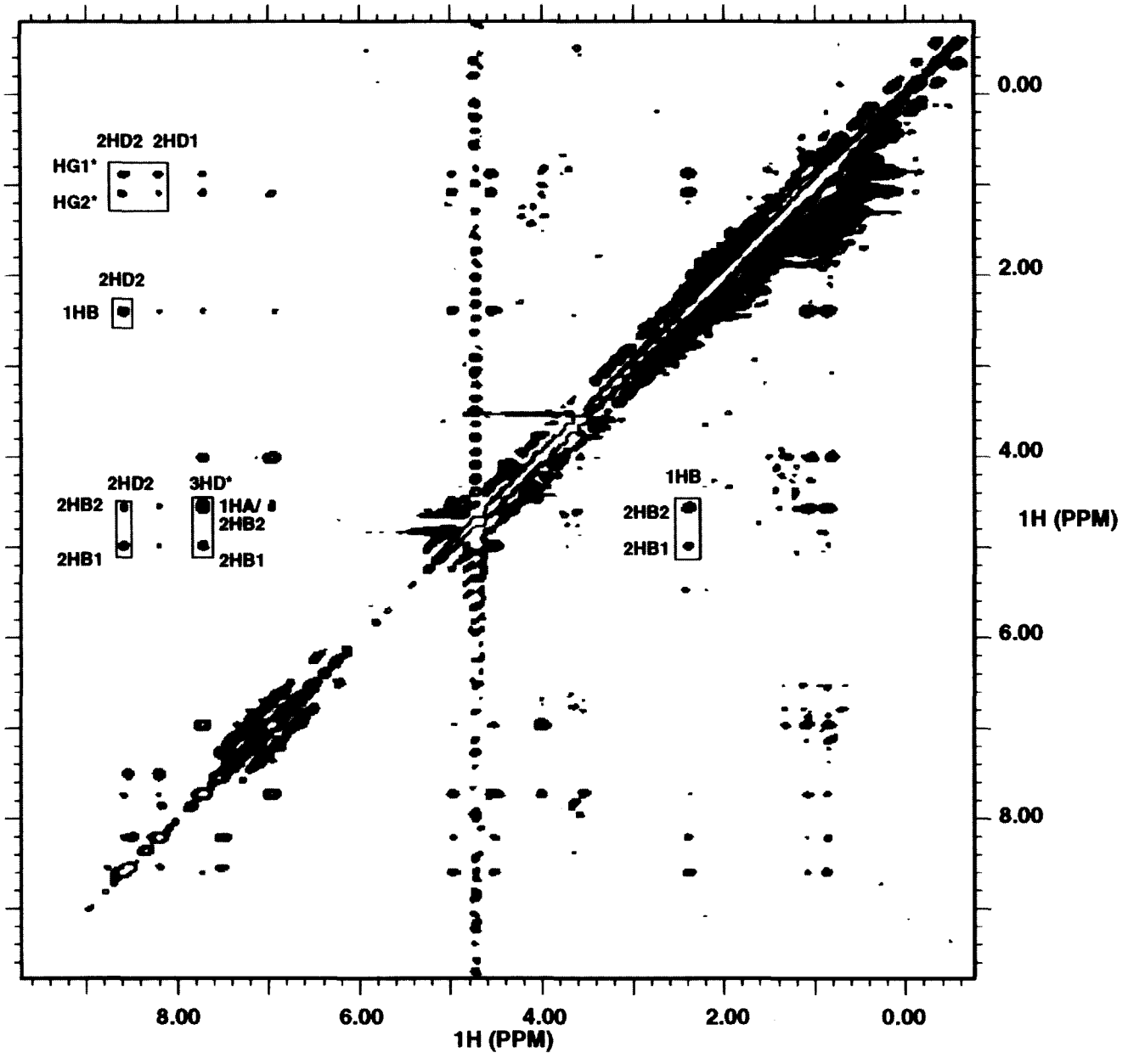

Figure 2. The $^{15}N/^{13}C$ filtered NOESY spectrum (120 ms mixing time) of the SCD–inhibitor complex in 100% D_2O–$Tris_{d11}$ buffer. Key NOE cross peaks used in defining the bound conformation of the inhibitor are labeled.

spectra were collected at five different mixing times and NOE buildup curves were generated for each of the inhibitor's proton resonances in order to exclude NOEs arising from spin diffusion effects. A list of distance constraints, used to calculate the bound conformation of the inhibitor, appears in Table 2. An ensemble of low energy structures was generated which satisfied the NOE distance constraints with no NOE violations greater than 0.2 Å. These calculated structures all showed association between the pyridyl and isopropyl methyl groups. The para-methoxy phenyl moiety was situated in an opposite orientation, as evidenced by the absence of NOE data between the methoxy phenyl group and either the pyridyl or isopropyl groups.

Determination of the binding mode of CGS 27023 (1) in stromelysin

Intermolecular NOE distance constraints used to accurately position the inhibitor in the enzyme's active site were obtained from ^{13}C-filtered NOESY and ^{15}N-edited NOESY spectra in either protonated or deuterated buffer. The NOEs observed between the inhibitor and stromelysin are summarized in Table 3. Two ^{13}C-filtered NOESY spectra, collected in 90% H_2O/ 10% D_2O–$Tris_{d11}$ buffer and 100% D_2O–$Tris_{d11}$ buffer are shown in Figure 3. The spectra highlight observed NOEs between the enzyme's amide protons and protons on the inhibitor which established key enzyme–inhibitor binding interactions. Slow deuterium

Table 2. NOE distance constraints used to calculate the bound conformation of the stromelysin inhibitor

Inhibitor protons	Upper bound (Å)	Inhibitor protons	Upper bound (Å)
1HB–HG2*	4	2HD2–1HB	3.8
1HB–HG1*	4	3HD1–3HH*	6
1HB–2HB1	5	3HD1–1HN	5
1HA–HG1*	4	3HD1–1HA	4
1HA–1HB	3.8	3HD1–1HO	5
1HA–HG2*	4	3HD2–2HB2	4
2HD1–2HB1	5	3HD2–2HB1	5
2HD1–2HZ	5	3HE1–3HH*	4.5
2HD1–HG1*	6	HG1*–1HO	6
2HD1–HG2*	5	2HB1–HG2*	6
2HD1–3HD2	5	2HB1–HG1*	6
2HD2–HG2*	6	2HB2–1HB	5
2HD2–HG1*	6	1HN–HG1*	6
2HD2–2HB2	5	1HN–HG2*	6
2HD2–2HB1	4	1HN–1HA	5
2HD2–3HD2	5	1HN–1HO	5

Table 3. Observed NOEs between the inhibitor and stromelysin

Inhibitor	(ppm)	(ppm)	Stromelysin
2HE1	7.51	8.31	HN Leu [164]
1HA	4.55	7.51	HN Ala [165]
3HD*	7.71	7.51	HN Ala [165]
HG2*	0.87	7.51	HN Ala [165]
1HO	14.57	7.07	HD2 His [201]
3HH*	3.96	12.74	HD1 His [201]
1HO	14.57	4.10	HA Glu [202]
1HO	14.57	1.53	HG* Glu [202]
3HE*	6.96	9.31	HN Glu [202]
3HH*	3.96	7.74	HN His [201]
3HE*	6.96	9.08	HN Tyr [223]
3HD*	7.71	9.08	HN Tyr [223]
1HN	11.82	5.12	HA His [166]

Hydrogen bonds/electrostatic interactions

Inhibitor	Stromelysin
SO_2	HN Leu [164]
HN	C=O Ala [165]
C=O	Zn
OH	Zn

exchange of amide protons in the SCD-inhibitor complex were essential in identifying hydrogen bonding interactions between the amide proton of Leu 164 and the sulfonamide oxygen on the inhibitor and between the carbonyl oxygen on Ala 165 and proton [1HN] on the inhibitor. These interactions were in complete agreement with orientation of the bound conformation to satisfy the experimentally determined NOE distance constraints. All conformational data were consistent with electrostatic interactions between the inhibitor's carbonyl and hydroxyl oxygen atoms and the catalytic zinc.

The docked structure of the stromelysin-inhibitor complex is shown in Figure 4. This complex was generated using the reported SCD structure,[12] and the bound conformation of **1** obtained from filtered NMR experiments. Orientation of this conformation, within the stromelysin binding site, was achieved by keeping the bound inhibitor conformation fixed, allowing flexibility of side chains in the enzyme's binding site, and minimizing to satisfy intermolecular NOE distance constraints between the enzyme and inhibitor. The NOE interactions between phenyl ring protons 3HE* and 3HD* and the amide proton of Tyr 223, and between the methoxy methyl protons 3HH* and the amide proton and ring proton [HD1] of His 201 established the orientation of the methoxy phenyl ring in the S1′ pocket of stromelysin. In addition, the NOE between the inhibitor's pyridyl ring proton 2HE1 and the amide proton of Leu 164 placed the pyridine ring in the enzyme's shallow S2′ pocket. Because the bound conformation of **1** fixed the orientation of the isopropyl methyl groups relative to the pyridine ring, the isopropyl group was automatically situated in the S1 pocket. An observed NOE from the isopropyl methyl group HG2* and the amide proton of Ala 165 was consistent with this orientation. Interactions of the inhibitor's hydroxyl proton [1HO] with proton HD2 on His 201 and protons HA and HG* on Glu 202 along with an NOE between the inhibitor's amide proton [1HN] and HA of His 166, fixed coordination of both the carbonyl oxygen and the hydroxyl oxygen with the catalytic zinc. Placement of the inhibitor to satisfy the intra and intermolecular NOE distance constraints also resulted in hydrogen bonding interactions between inhibitor proton [1HN] and the carbonyl oxygen of Ala 165, as well as the amide proton of Leu 164 and the sulfonamide oxygens on **1**. These hydrogen bonding and electrostatic interactions for the hydroxamic acid were corroborated by deuterium exchange studies and by X-ray studies of stromelysin-hydroxyamic acid complexes.[14] Compound **1** was one of the first potent, orally active stromelysin inhibitors discovered in this series. This NMR study rapidly established how this novel inhibitor binds to stromelysin.

Comparison of the CGS 27023-SCD binding mode with theoretical prediction in SCD and human fibroblast collagenase (HFC)

Molecular modeling calculations were performed to theoretically predict the potential binding modes of **1** in both stromelysin and collagenase. Energy minimization and Monte Carlo methods were used to dock **1** into the published crystal structures of either stromelysin[11] or human fibroblast collagenase (HFC).[19–22] For stromelysin, these modeling studies predicted the placement of the methoxy phenyl of **1** in the S1′ pocket as the most energetically favorable binding mode for this inhibitor. This binding mode was in complete agreement with the NMR derived structure. Molecular modeling studies with HFC, however, generated two energetically favorable binding modes for **1**. The first was similar to stromelysin placing the methoxy phenyl in the S1′ pocket of collagenase while the alternate binding mode

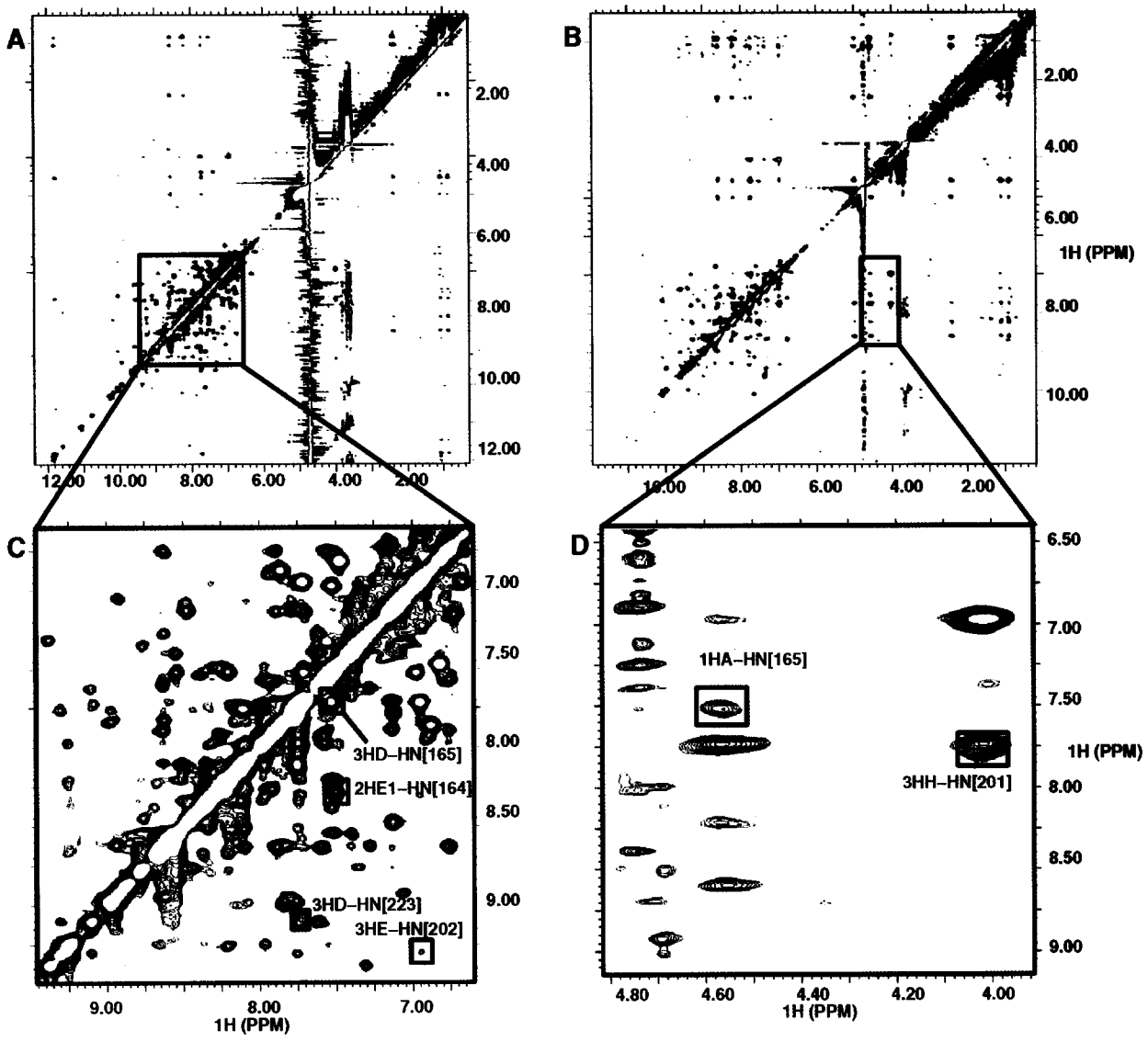

Figure 3. The ^{13}C filtered NOESY spectrum (150 ms mixing time) of the SCD-inhibitor complex. (A) The 2-D spectrum is recorded from a sample in 90% H_2O/10% D_2O–$Tris_{d11}$ buffer. (B) The 2-D spectrum is recorded from a sample in 100% D_2O–$Tris_{d11}$ buffer. (C) Expansion of the region shown in spectrum A. (D) Expansion of the region shown in spectrum B. Selected NOE cross peaks between protons on the unlabeled inhibitor and protons on the $^{13}C/^{15}N$ labeled protein are marked with a red box. These NOE cross peaks were used to define the orientation of the inhibitor in the enzyme's binding pocket.

placed the pyridine ring in the collagenase S1′ pocket and the methoxy phenyl ring in the S2′ pocket.

Since the catalytic binding sites of both stromelysin and collagenase possess structural similarities, speculation arose regarding the possibility that an alternate binding interaction of **1** with SCD may exist similar to that observed in collagenase. This uncertainty was corroborated by reports that the catalytic domain of stromelysin is able to assume variable conformations to accommodate a variety of inhibitor moieties.[14,17] Based on the specified sampling of conformational space used in these modeling studies, it was not clear whether alternate conformations of **1** or alternate binding interactions with SCD were indeed possible and needed to be considered. Our NMR data eliminated this uncertainty and unequivocally established the correct binding interaction of inhibitor **1** with stromelysin.

To investigate the binding site differences between the modeled stromelysin and collagenase complexes, structures representing the different binding modes of compound **1** complexed to SCD and HFC were superimposed (Fig. 5). Examination of the superimposed structures showed that compound **1** can extend more deeply into the S1′ pocket of SCD relative to HFC. This difference in binding interaction may be attributed to Arg 214 in collagenase, which protrudes into the S1′ pocket and effectively blocks deeper accessibility to the inhibitor. For stromelysin, however, Leu 197 occupies a similar position and leaves the S1′ channel open to solvent and accessible to inhibitor

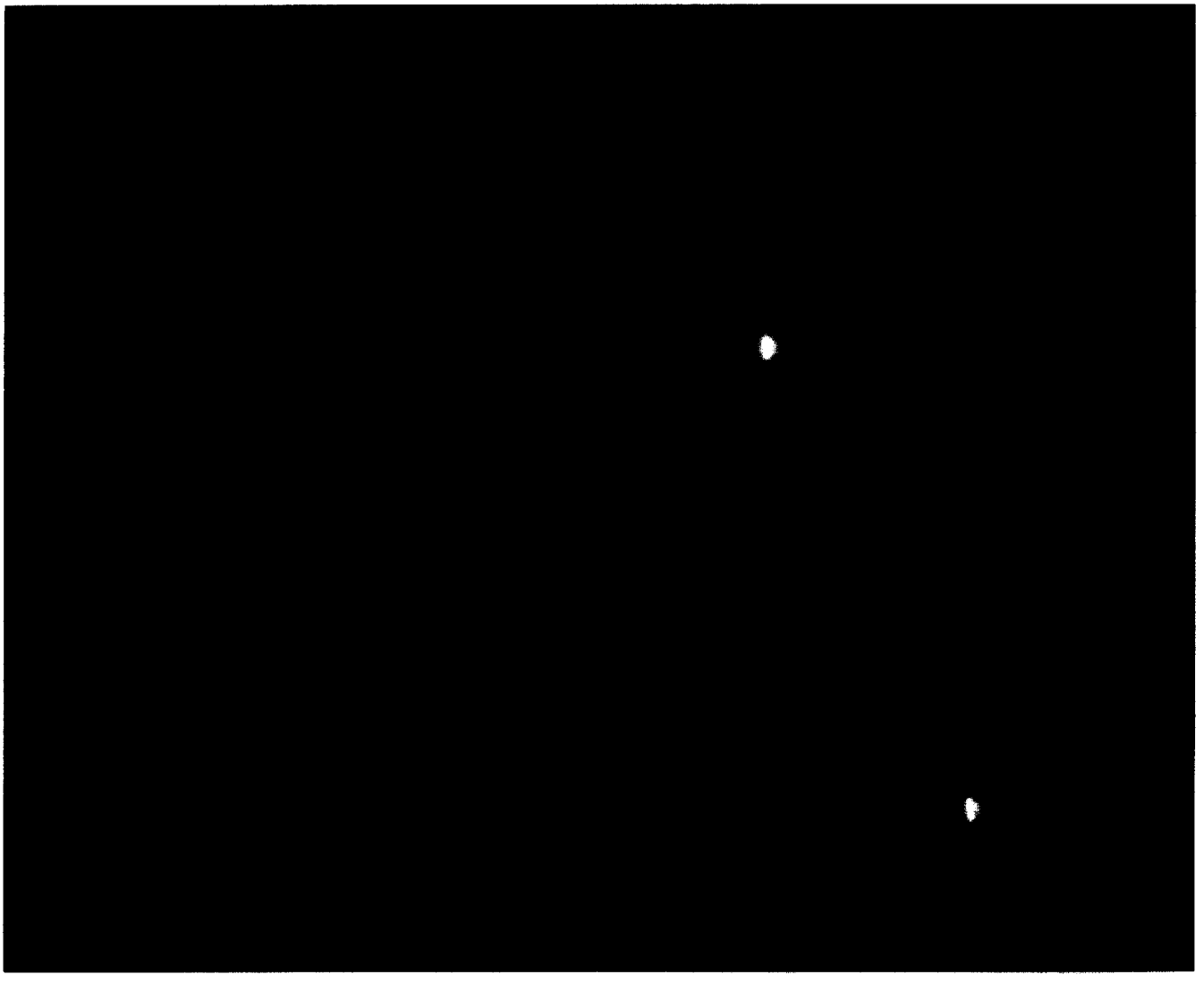

Figure 4. The active site of stromelysin (red) containing the inhibitor **1** (yellow). Both the catalytic and structural zinc atoms are displayed as green spheres. Distances between the enzyme and inhibitor are displayed which were derived from NOE data.

binding. Differences in the topology of the S2′ pocket in stromelysin vs. collagenase were also observed which may account for the alternate binding mode of **1** in collagenase. In particular, Leu 222 in stromelysin occupies a structurally equivalent position to Ser 239 in collagenase. Because the side chain methyl groups on Leu 222 extend into the S2′ pocket, this would result in van der Waals violations for a P2′ orientation of the methoxy phenyl group. Based on the theoretical model, such steric violations are not likely to occur in collagenase since the Ser 239 side chain points away from the binding cavity. This side chain orientation shifts the collagenase S2′ binding surface relative to stromelysin and results in directional accommodation of the methoxy phenyl group. Hence, accessibility of the S1′ pocket as well as directional orientation of S2′ relative to S1′ appear to be responsible for differences in the predicted binding modes of **1** in SCD vs. HFC.

Implications in drug design

The structural data obtained from these NMR experiments could be advantageously used to optimize the design of similar analogues of **1**. In particular, knowledge that the methoxy phenyl group occupies the S1′ region could be used to modify this moiety or to design a unique P1′ portion of the inhibitor that can extend into the long, narrow, hydrophobic binding pocket, thereby enhancing interaction with the enzyme. Likewise, interactions of the pyridyl ring in the shallow S2′ pocket of SCD presented possibilities for specific inhibitor modifications. The isopropyl group, however, extends into the S1 binding pocket, which is primarily comprised of a wide hydrophobic surface. Since the enzyme–inhibitor complex leaves the isopropyl methyl groups solvent exposed, it was expected that synthetic changes to this portion of the molecule would be well tolerated by a wide variety of chemical substitutions.

Figure 5. Stereo view (relaxed eye) of the superposition of modeled structures of stromelysin and collagenase complexed to inhibitor **1**. Stromelysin is shown in green with the corresponding inhibitor in white, while collagenase appears in pink with the corresponding inhibitor shown in red. The alternate binding mode for **1** (red) found in collagenase, shows the pyridine ring in the S1′ pocket and the methoxy phenyl group in S2′. Based on this theoretical model, steric interactions with Leu 222 would exclude this binding mode in stromelysin. Comparison of the stromelysin and collagenase binding sites shows the side chains of collagenase, Arg 214 and Asn 180, pointing toward the binding cavity while Ser 239 points away from the binding site. Unlike Arg 214 in collagenase, stromelysin's structural equivalent, Leu 197, does not extend into the S1′ pocket leaving this region open and accessible to inhibitor binding. The stromelysin side chain of Leu 222 points toward the S2′ pocket and Val 163 points away from the binding site which are opposite to that of Ser 239 and Asn 180 in collagenase, respectively. These differences define the accessible binding surfaces for both enzymes.

The structure–activity relationship for a number of P1 substituted analogues of compound **1** supported this hypothesis.[23] Major structural changes to the P1 region resulted in similar or slightly enhanced binding constants, hence these results suggest that the observed increases in activity may be attributed to general protein binding.

Conclusion

The biologically active conformation of a novel and very potent stromelysin inhibitor has been determined by NMR spectroscopy. Docking studies using the bound conformation of **1** and intermolecular NOE distance constraints showed that the inhibitor's methoxy phenyl group occupies the S1′ pocket of stromelysin, the major site of hydrophobic enzyme–inhibitor interaction, while the pyridine ring is situated in the shallow S2′ pocket and the isopropyl methyl groups reside in the solvent accessible S1 pocket. The inhibitor's bound conformation and enzyme binding interactions were corroborated by molecular modeling predictions. This study provided the first three dimensional structure of a nonpeptidic stromelysin inhibitor that could be used in the design of more potent inhibitors in this series.

Experimental

Sample preparation of $^{13}C/^{15}N$-labeled stromelysin. Recombinant BL21(DE3) *E. coli* containing the plasmid specifying truncated pro-stromelysin was grown in M9 minimal media using 99% $^{15}NH_4Cl$ and 96% ^{13}C-6 glucose as the sole nitrogen and carbon sources respectively. Pro-stromelysin was purified according to published procedures.[10] The protein was subsequently activated by heating the sample at 52 °C for 4 h. The activated stromelysin was further purified using a Mono S column eluting with 20 mM MES buffer (pH 6.5), 5 mM $CaCl_2$, and 0.02% NaN_3. Pure activated stromelysin was obtained from wash fractions. The NMR samples were prepared by concentrating protein to 0.5–1.0 mM using Centricon tubes with an exchange buffer (20 mM $Tris_{d11}$–HCl, pH 6.8, 20 mM $CaCl_2$, 0.02% NaN_3 in 90% H_2O/10% D_2O or 100% D_2O). The enzyme was inhibited with 2 mM inhibitor and excess inhibitor was removed using Centricon filtration.

NMR. The NMR spectra were acquired on a Bruker DMX-600 NMR spectrometer at 25 °C and 37 °C. Proton, carbon and nitrogen resonance assignments of stromelysin were made from the following experiments: 2-D ^1H-^{15}N HSQC,[24] 2-D ^1H-^{13}C HSQC,[25] 3-D CBCA(CO)NH,[26] 3-D HBHA-(CO)NH,[27] 3-D HNCA,[28] 3-D HNHA[29] and 3-D HCCH-TOCSY.[30,31] The inhibitor resonances were assigned from 2-D ^{13}C-filtered COSY and 2-D $^{13}C/^{15}N$-filtered NOESY spectra.[32,33] Intramolecular NOE assignments for the inhibitor were made from $^{13}C/^{15}N$-filtered NOESY spectra acquired at mixing times of 60, 90, 120, 150, and 180 ms. NOE buildup curves were generated for each proton to identify

those NOEs resulting from spin diffusion effects. Intermolecular NOEs between stromelysin and the inhibitor were assigned from 3-D ^{15}N-edited NOESY[34] and 2-D ^{13}C-filtered NOESY spectra. All 3-D data were transformed and processed on a Silicon Graphics (Onyx) workstation using the Felix software (MSI, Burlington, MA), with zero filling in each dimension. All 2-D data were processed on a Bruker DMX-600 NMR spectrometer. Data analysis was carried out on Silicon Graphics workstations using NMRCOMPASS software (MSI, Burlington, MA).

Structure calculation. Structure calculations were carried out on a Silicon Graphics Onyx workstation using the X-plor[35] program. Randomly sampled structures of the inhibitor were subjected to simulated annealing and refined using 32 intramolecular NOE distance constraints. An ensemble of the ten lowest energy structures showed no distance violations greater than 0.2 Å. The resultant bound conformation was manually docked into the reported stromelysin binding site[12] using Quanta (MSI, Burlington, MA). The docked structure was energy minimized using the CHARMM[36] force field employing the Adopted Basis Newton–Raphson function with an energy gradient tolerance of 0.01, an initial step size of 0.02 Å, 2000 steps and applying 13 intermolecular NOE distance constraints between the inhibitor and the enzyme. All atoms were held fixed with the exception of side chains and flexible loop regions surrounding the enzyme's binding site (residues 162–165, 221–224 and 202–204).

Molecular modeling. Computational docking was carried out on an SGI Onyx workstation using the MCDOCK procedure of the QXP program (Quick eXPlore).[37] QXP contains routines for torsion space and Cartesian space docking, searching and minimization; a variant of the AMBER* forcefield[38,39] of MacroModel[40] was used. Inhibitor docking was carried out using a truncated model shell of each enzyme crystal structure spanning approximately a 7 Å radius from the enzyme's active site. All enzyme shell residues were held fixed with the exception of residues whose mobility was verified via temperature factors and molecular dynamics, namely Leu 164, His 201, Glu 202, His 205, His 211, Leu 222, and Tyr 223 in stromelysin, and residues Asn 180 (side chain only), Leu 181, Tyr 210, Val 215, Glu 219, Pro 238, and Ser 239 in collagenase. Unfixed shell residues were permitted unlimited torsional rotation. The inhibitor's hydroxamate carbonyl and hydroxyl oxygen atoms were tethered to the catalytic zinc using zero-order bonds (biasing the binding mode by known zinc interactions) while the remainder of the molecule was allowed to rotate and translate freely during the docking computation. QXP computation typically sampled 1000–5000 docked conformations, ranking and reporting 25–50 of the complexes with the best docked assessment energies. Visualization of the modeled structures and accessible surfaces[41] was performed with MacroModel version 5.5.[40]

Acknowledgements

The authors wish to thank Dr David Parker for the inhibitor (CGS 27023).

References

1. Murphy, G.; Hembry, R. M.; Reynolds, J. *J. Collagen Relat. Res.* **1986**, *6*, 351.

2. Flannery, C.; Lark, M. W.; Sandt, J. D. *J. Biol. Chem.* **1992**, *267*, 1008.

3. Stetler-Stevenson, W. G.; Liotta, L. A.; Kleiner, Jr. D. E. *FASEB J.* **1993**, *7*, 1434.

4. Greenwald, R. A.; Golub, L. M., Eds.; In *Inhibition of Matrix Metalloproteinases: Therapeutic Potential*; Ann. N.Y. Acad. Sci.: New York, 1994; Vol. 732.

5. Okada,Y.; Nakanishi, I. *FEBS Lett.* **1989**, *249*, 353.

6. Okada, Y.; Nagase, H.; Harris, E. D. *J. Biol. Chem.* **1986**, *261*, 14245.

7. Okada, Y.; Harris, E. D.; Nagase, H. *Biochem. J.* **1988**, *254*, 731.

8. Murphy, G.; Cockett, M. I.; Stephens, P. E.; Smith, B. J.; Docherty, A. J. P. *Biochem. J.* **1987**, *248*, 265.

9. Nagase, H.; Enghild, J. J.; Suzuki, K.; Salvesen, G. *Biochemistry* **1990**, *29*, 5783.

10. Marcy, A. I.; Eiberger, L. L.; Harrison, R.; Chan, H. K.; Hutchinson, N. I.; Hagmann, W. K.; Cameron, P. M.; Boulton, D. A; Hermes, J. D. *Biochemistry* **1991**, *30*, 6476.

11. Becker, J. W.; Marcy, A. I.; Rokosz, L. L.; Axel, M. G.; Burbaum, J. J.; Fitzgerald, P. M. D.; Cameron, P. M.; Esser, C. K.; Hagmann, W. K.; Hermes, J. D.; Springer, J. P. *Protein Sci.* **1995**, *4*, 1966.

12. Gooley, P. R.; O'Connell, J. F.; Marcy, A. I.; Cuca, G. C.; Salowe, S. P.; Bush, B. L.; Hermes, J. D.; Esser, C. K.; Hagmann, W. K.; Springer, J. P.; Johnson, B. A. *Nature Struct. Biol.* **1994**, *1*, 111.

13. Van Doren, S. R.; Kurochkin, A. V.; Hu, W.; Ye, Q.; Johnson, L. L.; Hupe, D. J.; Zuiderweg, E. R. P. *Protein Sci.* **1995**, *4*, 2487.

14. Dhanaraj, V.; Ye, Q.-Z; Johnson, L. L.; Hupe, D. J.; Ortwine, D. F.; Dunbar, Jr. J. B.; Rubin, R. J.; Pavlovsky, A.; Humblet, C.; Blundell, T. L. *Structure* **1996**, *4*, 375.

15. Van Doren, S. R.; Kurochkin, A. V.; Ye, Q.; Johnson, L. L.; Hupe, D. J.; Zuiderweg, E. R. P. *Biochemistry* **1992**, *32*, 13109.

16. Gooley, P. R.; Johnson, B. A.; Marcy, A. I.; Cuca, G. C.; Salowe, S. P.; Hagmann, W. K.; Esser, C. K.; Springer, J. P. *Biochemistry* **1993**, *32*, 13098.

17. Rockwell, A.; Melden, M.; Copeland, R. A.; Hardman, K.; Decicco, C. P.; DeGrado, W. F. *J. Am. Chem. Soc.* **1996**, *118*, 10337.

18. MacPherson, L. J.; Parker, D. T. US Patent No. 5 455 258, **1995**.

19. Borkakoti, N.; Winkler, F. K.; Williams, D. H.; D'Arcy, A.; Broadhurst, M. J.; Brown, P. A.; Johnson, W. H.; Murray, E. J. *Nature (London) Struct. Biol.* **1994**, *1*, 106.

20. Lovejoy, B.; Cleasby, A.; Hassell, A. M.; Longley, K.; Luther, M. A.; Weigl, D.; McGeehan, G.; McElroy, A. B.;

Drewry, D.; Lambert, M. H.; Jordan, S. R. *Science* **1994**, *263*, 375.

21. Lovejoy, B.; Hassell, A. M.; Luther, M. A.; Weigl, D.; Jordan, S. R. *Biochemistry* **1994**, *33*, 8207.

22. Spurlino, L.; Smallwood, A. M.; Carlton, D. D.; Banks, T. M.; Vavra, K. J.; Johnson, J. S.; Cook, E. R.; Falvo, J.; Wahl, R. C.; Pulvino, T. A.; Wendolski, J. J.; Smith, D. L. *Proteins* **1994**, *19*, 98.

23. MacPherson, L. J.; Bayburt, E. K.; Capparelli, M. P.; Carroll, B. J.; Goldstein, R.; Justice, R. J.; Zhu, L.; Hu, S.; Melton, R. A.; Fryer, L.; Goldberg, R. L.; Doughty, R. J.; Spirito, S.; Blancuzzi, V.; Wilson, D.; O'Byrne, E. M.; Ganu, V.; Parker, D. T. *J. Med. Chem.* **1997**, *40*, 2525.

24. Bodenhausen, G.; Ruben, D. J. *J. Phys. Lett.* **1980**, *69*, 185.

25. Vuister, G. W.; Bax, A. *J. Magn. Reson.* **1992**, *98*, 428.

26. Grzesiek, S.; Bax, A. *J. Magn. Reson.* **1992**, *99*, 201.

27. Grzesiek, S.; Bax, A. *J. Biomol. NMR.* **1993**, *3*, 185.

28. Grzesiek, S.; Bax, A. *J. Magn. Reson.* **1992**, *96*, 432.

29. Vuister, G. W.; Bax, A. *J. Am. Chem. Soc.* **1993**, *115*, 7772.

30. Bax, A.; Clore, G. M.; Gronenborn, A. *J. Magn. Reson.* **1990**, *88*, 425.

31. Fesik, S. W.; Eaton, H. L.; Olejniczak, E. T.; Zuiderweg, E. R. P.; McIntosh, L. P.; Dahlquist, F. W. *J. Am. Chem. Soc.* **1990**, 112, 886.

(*Reveived in U.S.A.* 22 *April* 1997; *accepted* 14 *July* 1997)

32. Otting, G.; Wuthrich, K. *Q. Rev. Biophys.* **1990**, *23*, 39.

33. Bax, A.; Vuister, G. W.; Grzesiek, S.; Delaglio, F.; Wang, A. C.; Tschudin, R.; Zhu, G. *Methods Enzymol.* **1994**, *239*, 79.

34. Marion, D.; Kay, L. E.; Sparks, S. W.; Torchia, D. A.; Bax, A. *J. Am. Chem. Soc.* **1989**, *111*, 1515.

35. Brunger, A. T. X-PLOR Version 3.1 Yale University: New Haven, CT, **1993**.

36. Brooks, B. R.; Bruccoleri, R. E.; Olafson, B. D.; States, D. J.; Swaminathan, S.; Karplus, M. *J. Comput. Chem.* **1983**, *4*, 187.

37. McMartin, C.; Bohacek, R. *J. Comput. Aided Mol. Design* **1995**, *9*, 237.

38. Weiner, S. J.; Kollman, P. A.; Case, D. A.; Singh, U. C.; Ghio, C.; Alagona, G.; Profeta, S.; Weiner, P. *J. Am. Chem. Soc.* **1984**, *106*, 765.

39. Weiner, S. J.; Kollman, P. A.; Nguyen, D. T.; Case, D. A. *J. Comp. Chem.* **1986**, *7*, 230.

40. Mohamadi, F.; Richards, N. G. J.; Guida, W. C.; Liskamp, R.; Lipton, M.; Caufield, C.; Chang, G.; Hendrickson, T.; Still, W. C. *J.Comput. Chem.* **1990**, *11*, 440. MacroModel/Batchmin is available from Professor W. Clark Still, Dept. of Chemistry, Columbia University, NY, NY 10027.

41. Bohacek, R. S.; McMartin, C. *J. Med. Chem.* **1992**, *35*, 1671.